Electronic Supplementary Information (ESI)

A New Approach for the Facile Preparation of Metal–Organic Framework Composites Directly Contacting with Metal Nanoparticles through Arc Plasma Deposition

Masaaki Sadakiyo,*,† Shotaro Yoshimaru,‡ Hidetaka Kasai,# Kenichi Kato,# Masaki Takata,#
Miho Yamauchi*,†,‡

† International Institute for Carbon-Neutral Energy Research (WPI-I2CNER), Kyushu University, 744 Moto-oka, Nishi-ku Fukuoka 819-0395, Japan. ‡ Department of Chemistry, Faculty of Science, Kyushu University, 744 Moto-oka, Nishi-ku Fukuoka 819-0395, Japan. # RIKEN SPring-8 Center, 1-1-1 Kouto, Sayo-cho, Sayo-gun, Hyogo 679-5148, Japan.

E-mail: sadakiyo@i2cner.kyushu-u.ac.jp; yamauchi@i2cner.kyushu-u.ac.jp

Preparation of support materials

Synthesis of ZIF-8 ($\{Zn(mim)_2\}_\infty$ (mim^- = 2-methylimidazolate))

The ZIF-8 support was synthesised by mixing a methanol solution of $Zn(NO_3)_2 \cdot 6H_2O$ (50 mmol, 14.88 g dissolved in 500 ml methanol) and Hmim (200 mmol, 16.42 g dissolved in 500 ml methanol). The mixture was kept at room temperature for 24 h without stirring. The white precipitate was then collected by centrifugation and washed by repeated dispersion in methanol solvent and centrifugation. The washed sample was then dried under vacuum at room temperature.

Synthesis of MIL-101 ($\{Cr_3(NO_3)(H_2O)_2O(bdc)_3\}_\infty$ (bdc^- = 1,4-benzenedicarboxylate))

The MIL-101 support was synthesised by heating a mixture of $Cr(NO_3)_3 \cdot 9H_2O$ (40 mmol, 16.0 g), terephthalic acid (40 mmol, 6.64 g), and distilled water (160 ml) (mixture was separately filled in several small Teflon-lined autoclaves) at 218 °C for 18 h. The precipitate was collected by centrifugation and washed with distilled water. The sample was stirred in DMF at 75 °C for 3 h and collected by centrifugation. The precipitate was then washed by repeated dispersion in solvent and centrifugation (DMF, methanol, and acetone were used as washing solvents) and then dried under vacuum at room temperature.

Synthesis of UiO-66-NH$_2$ ($\{Zr(bdc\text{-}NH_2)_2\}_\infty$ ($bdc\text{-}NH_2^-$ = 2-amino-1,4-benzenedicarboxylate))

The UiO-66-NH$_2$ support was synthesised by heating a mixture of $ZrCl_4$ (8.2 mmol, 1.92 g), 2-aminoterephthalic acid (8.2 mmol, 1.49 g), and DMF (480 ml) in a glass bottle at 120 °C for 24 h. The yellow precipitate was collected by centrifugation and washed with DMF. It was further washed by repeated dispersion in MeOH and centrifugation several times. After that, the powder was then dried under vacuum at 160 °C over a night.

Synthesis of Zn-MOF-74 ($\{Zn_2(dobtc)\}_\infty$ ($dobtc^{4-}$ = 2,5-dioxidoterephthalate))

The Zn-MOF-74 support was synthesised by heating a mixture of $Zn(NO_3)_2 \cdot 6H_2O$ (114 mmol, 33.91 g), 2,5-dihydroxyterephthalic acid (39 mmol, 7.73 g), distilled water (75 ml), and DMF (1500 ml) in a glass bottle at 100 °C for 20 h without stirring. The yellow precipitate was filtered and washed with DMF and water. It was then refluxed in MeOH for four days (solvent was exchanged with fresh MeOH several times). The sample was filtered and washed with MeOH and dried under vacuum at room temperature.

Preparation of M/MOFs

M/MOFs (M = Pt, Pd, and Ru; MOFs = ZIF-8, MIL-101, UiO-66-NH$_2$, and Zn-MOF-74) were prepared by irradiating plasma shots from arc plasma guns (ULVAC ADP-3P-N2) equipping each metal onto the

MOF supports in a vacuum chamber. First, several grams of the support were put in a pot in the vacuum chamber. Several tens of thousands of plasma shots were showered onto the MOF supports, as listed in Table S1 with 1–2 Hz frequency under vacuum at the applied voltage of 140 V except the Pt/Zn-MOF-74 (both 90 and 140 V was applied for observation of particle growth). The sample was continuously stirred by the combination of stirrer bar and rotation of the pot during the deposition process. The pot was maintained at 18 °C using a water-cooling apparatus.

Table S1. Support amounts and shot numbers for APD preparation

Sample	Pt/ZIF-8	Pd/ZIF-8	Ru/ZIF-8	Ru/ MIL-101	Pd/ UiO-66-NH_2	Pt/ Zn-MOF-74	Pt–Co/ ZIF-8
Support (g)	4.55	4.57	4.55	1.90	3.07	5.20	4.58
Shot ($\times 10^2$)	100	88	434	270	170	0~400	230

Preparation of Pd-PVP/UiO-66-NH_2 (PVP = poly (N-vinyl-2-pyrrolidone))

An aqueous solution of 2.0 mM H_2PdCl_4 was prepared by mixing of $PdCl_2$ (0.3 mmol, 53.2 mg), 0.2 M aqueous solution of HCl (3 ml), and H_2O (147 ml). PVP-coated Pd NPs (**Pd-PVP**) were prepared by reflux of a mixture of the H_2PdCl_4 (45 ml of 2.0 mM*aq*), PVP K30 (3.6 mmol, 144 mg), distilled water (75 ml), and ethanol (30 ml) for 3 h with stirring. Then, the solvent and included HCl was removed by evaporation. The dried precipitate was dispersed in methanol (50 ml). It was added into a suspension of UiO-66-NH_2 (480 mg) dispersed in methanol (50 ml). After sonication, the solution was put on a water bath and the solvent was completely evaporated with vigorous stirring by heating.

Measurements

X-ray powder diffraction (XRPD) was performed using the RIKEN Materials Science beamline BL44B2 at SPring-8 (λ = 1.080 Å). Inductively coupled plasma atomic emission spectrometry (ICP-AES) was performed using Thermo-Fisher iCAP6300. Scanning transmission electron microscopy (STEM) observations and STEM combined with EDS (STEM–EDS) analyses were carried out with a JEOL JEM-ARM 200F operated at 200 kV accelerating voltage. The mean diameters and size distributions are estimated by counting more than 200 particles. Samples were dried at room temperature under vacuum overnight, then adsorption/desorption isotherms of N_2 were measured with a BELSORP-max (MicrotracBEL, Inc.) instrument at 77 K. X-ray photoelectron spectroscopy (XPS) was performed using ULVAC-PHI PHI 5000 Versa Probe-II with a Al-$K\alpha$ X-ray source. The XPS spectra were calibrated using a C1s peak at 284.5 eV. According to previous literatures,[1] XPS peaks were attributed to M^0 (M = Pt, Pd, or Ru), M^{2+} (Pt or Pd), or M^{4+} (Ru) components. Note that the sample including Pt or Pd showed an additional peak located at slightly lower binding energy (e.g. 72.9 eV for Pt) than divalent oxides (e.g. 71.8 eV for Pt), such as PtO or PdO. We suppose that these peaks are attributable to the divalent ions coordinated by the ligands located on the surface of MOF crystals.

(Reference 1) (a) J. Z. Shyu, K. Otto, *Appl. Sur. Sci.*, 1988, **32**, 246–252. (b) K. R. Priolkar, P. Bera, P. R. Sarode, M. S. Hegde, S. Emura, R. Kumashiro, N. P. Lalla, *Chem. Mater.*, 2002, **14**, 2120–2128. (c) J. L. G. Fuente, M. V. M. Huerta, S. Rojas, P. H. Fernandez, P. Terreros, J. L. G. Fierro, M. A. Pena, *Appl. Catal. B*, 2009, **88**, 505–514.

Catalytic reaction

The formic acid decomposition reaction was conducted using 50–73 mg of the prepared catalysts. The catalyst and 50 ml of water were placed inside a reaction vessel connected with the closed-circuit apparatus. The argon gas (approx. 50 mmHg) was purged after the air was removed. The reaction vessel was kept at 50 °C. 0.15 ml (3.97 mmol) of formic acid was introduced into the reaction vessel using a syringe at the beginning of the reaction. The amount of produced H_2 was monitored every 20 minutes by Shimadzu GC-8A gas chromatograph equipping MS-5A column within 3 hours.

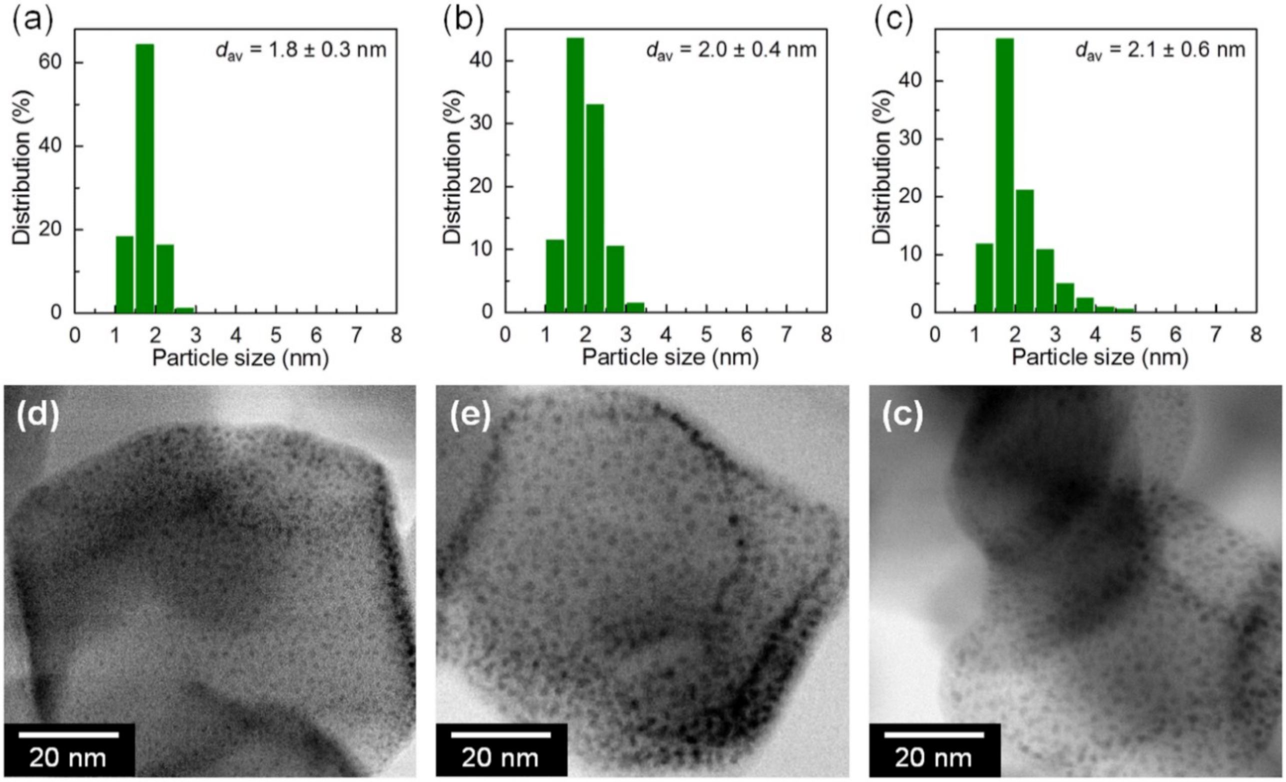

Fig. S1 Particle-size distributions of (a) **Pt/ZIF-8**, (b) **Pd/ZIF-8**, and (c) **Ru/ZIF-8**. Additional STEM images of (d) **Pt/ZIF-8**, (e) **Pd/ZIF-8**, (f) **Ru/ZIF-8**.

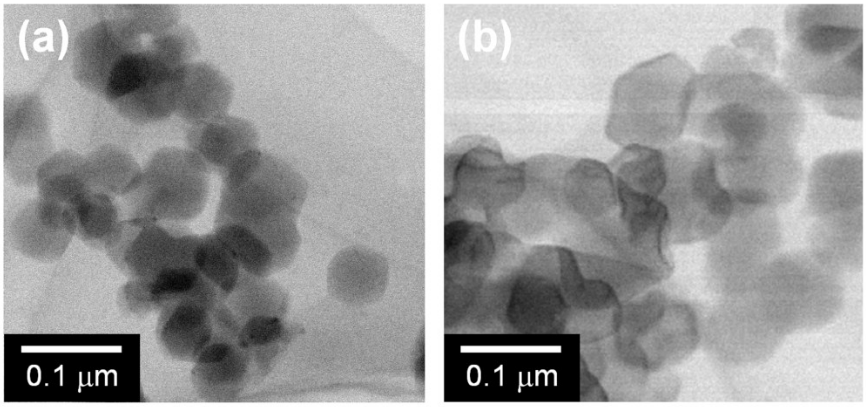

Fig. S2 STEM images of (a) blank ZIF-8 and (b) **Pt/ZIF-8**. The dark contrast around the ZIF-8 crystal in **Pt/ZIF-8** is due to the deposited Pt, while there are some bare ZIF-8 crystals.

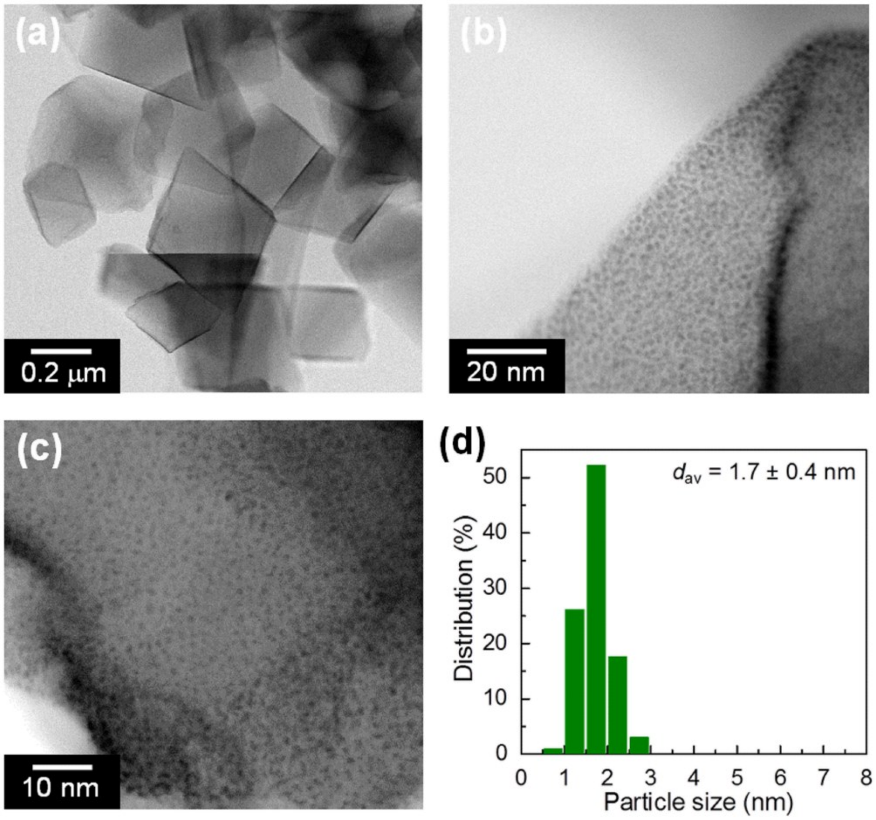

Fig. S3 (a, b, c) STEM images and (d) size distribution of **Ru/MIL-101**.

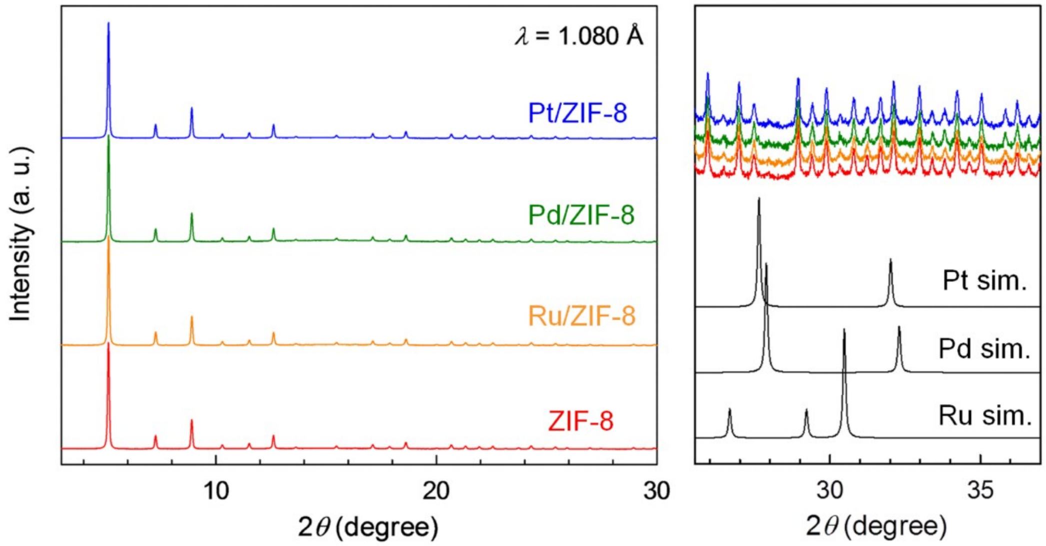

Fig. S4 (left) XRPD patterns of **Pt/ZIF-8**, **Pd/ZIF-8**, **Ru/ZIF-8**, and blank ZIF-8 at room temperature. (right) Magnified XRPD patterns with simulated patterns of bulk Pt (fcc), Pd (fcc), and Ru (hcp). Blue, green, orange, and red correspond to **Pt/ZIF-8**, **Pd/ZIF-8**, **Ru/ZIF-8**, and blank ZIF-8, respectively.

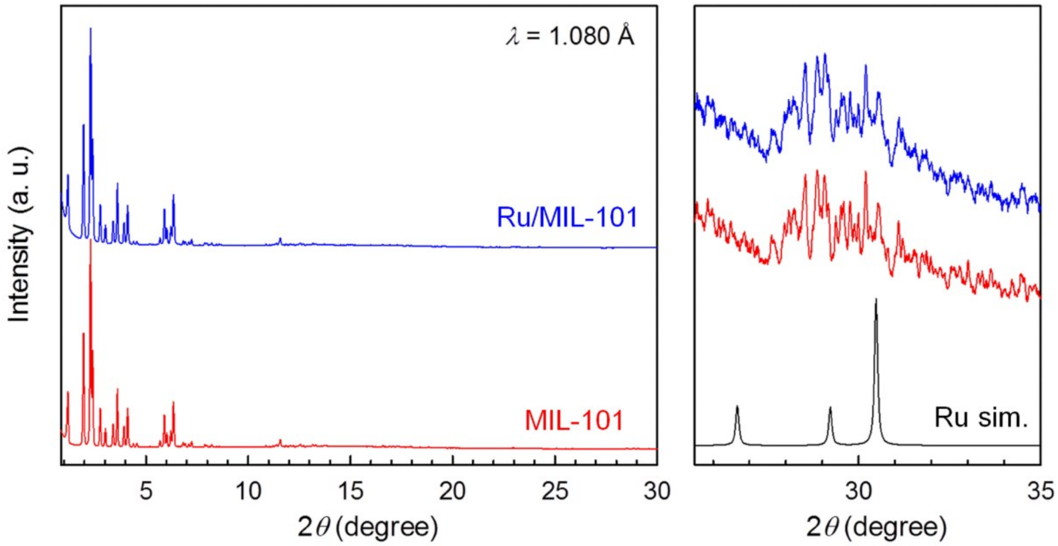

Fig. S5 (left) XRPD patterns of **Ru/MIL-101**, and blank MIL-101 at room temperature. (right) Magnified XRPD patterns with simulated pattern of bulk Ru (hcp). Blue and red correspond to **Ru/MIL-101** and blank MIL-101, respectively.

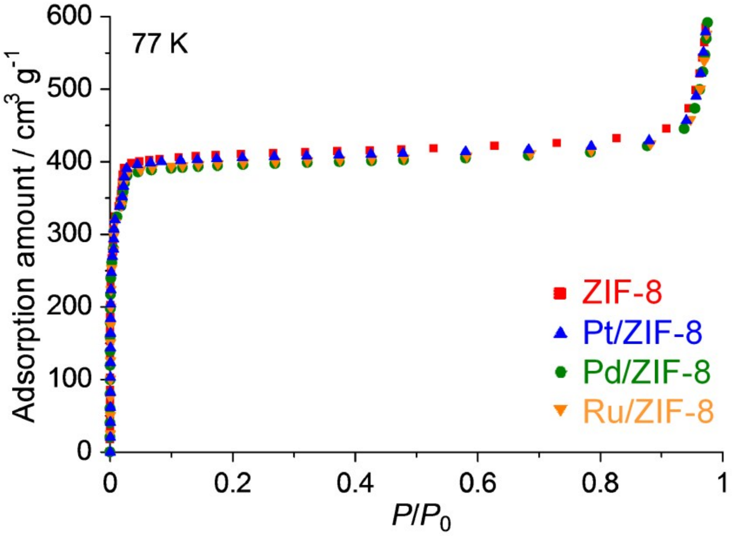

Fig. S6 N_2 adsorption isotherms of (blue) **Pt/ZIF-8**, (green) **Pd/ZIF-8**, (orange) **Ru/ZIF-8**, and (red) blank ZIF-8 at 77 K.

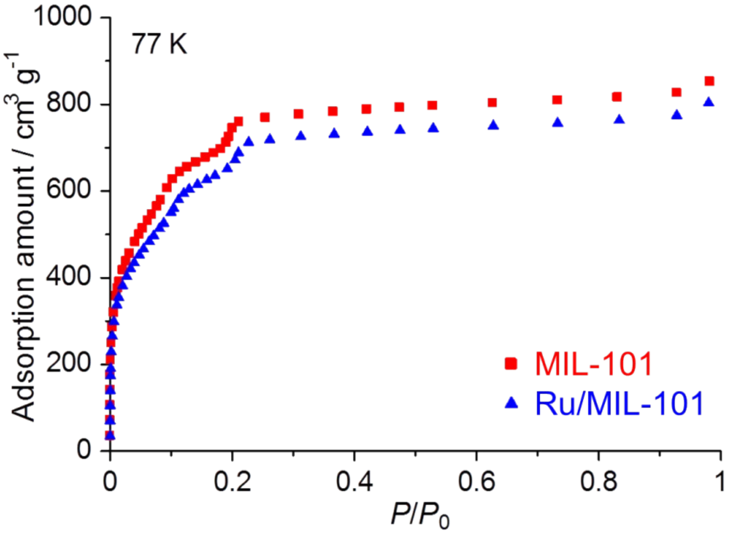

Fig. S7 N_2 adsorption isotherms of (blue) **Ru/MIL-101** and (red) blank MIL-101 at 77 K.

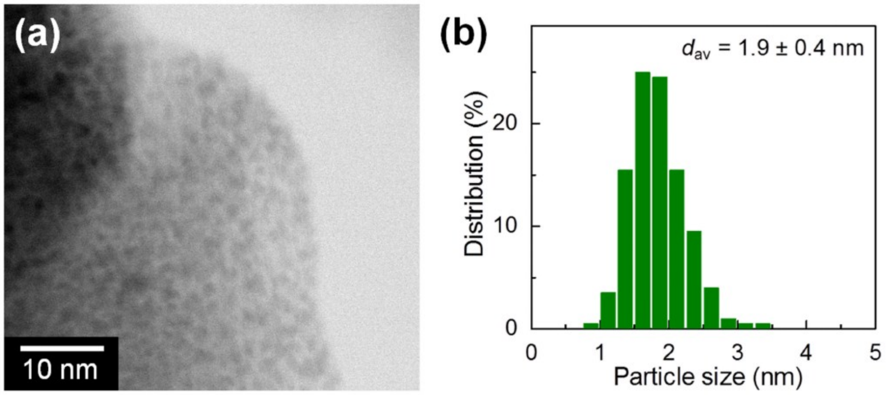

Fig. S8 (a) STEM image and (b) size distribution of **Pd/UiO-66-NH$_2$**.

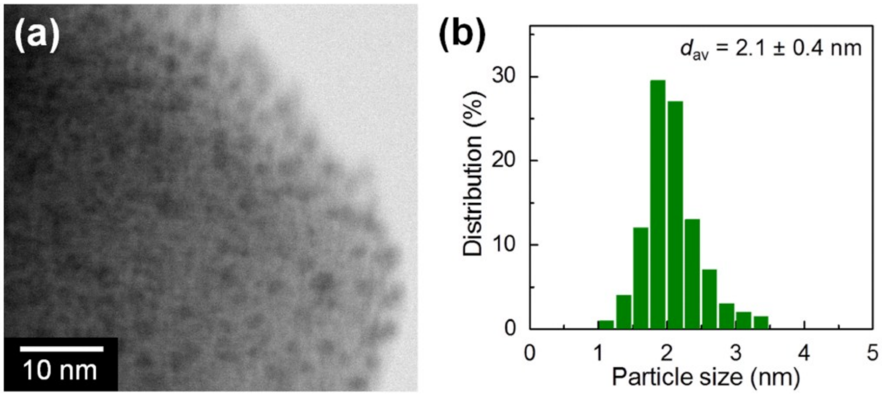

Fig. S9 (a) STEM image and (b) size distribution of **Pd-PVP/UiO-66-NH$_2$**.

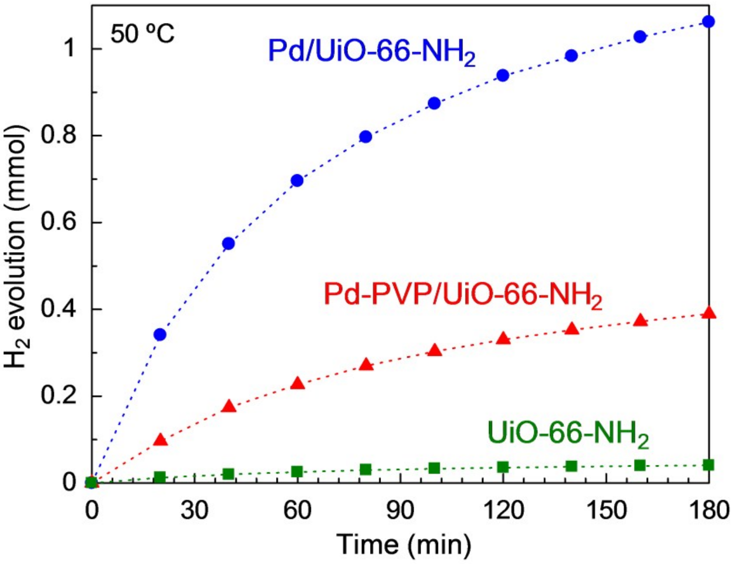

Fig. S10 H$_2$ production from formic acid using different catalysts of (blue) **Pd/UiO-66-NH$_2$** (50 mg, the amount of Pd is 0.55 mg) prepared through the APD method, (red) **Pd-PVP/UiO-66-NH$_2$**, (73 mg, the amount of Pd is 0.60 mg), (green) UiO-66-NH$_2$ (50 mg, no Pd).

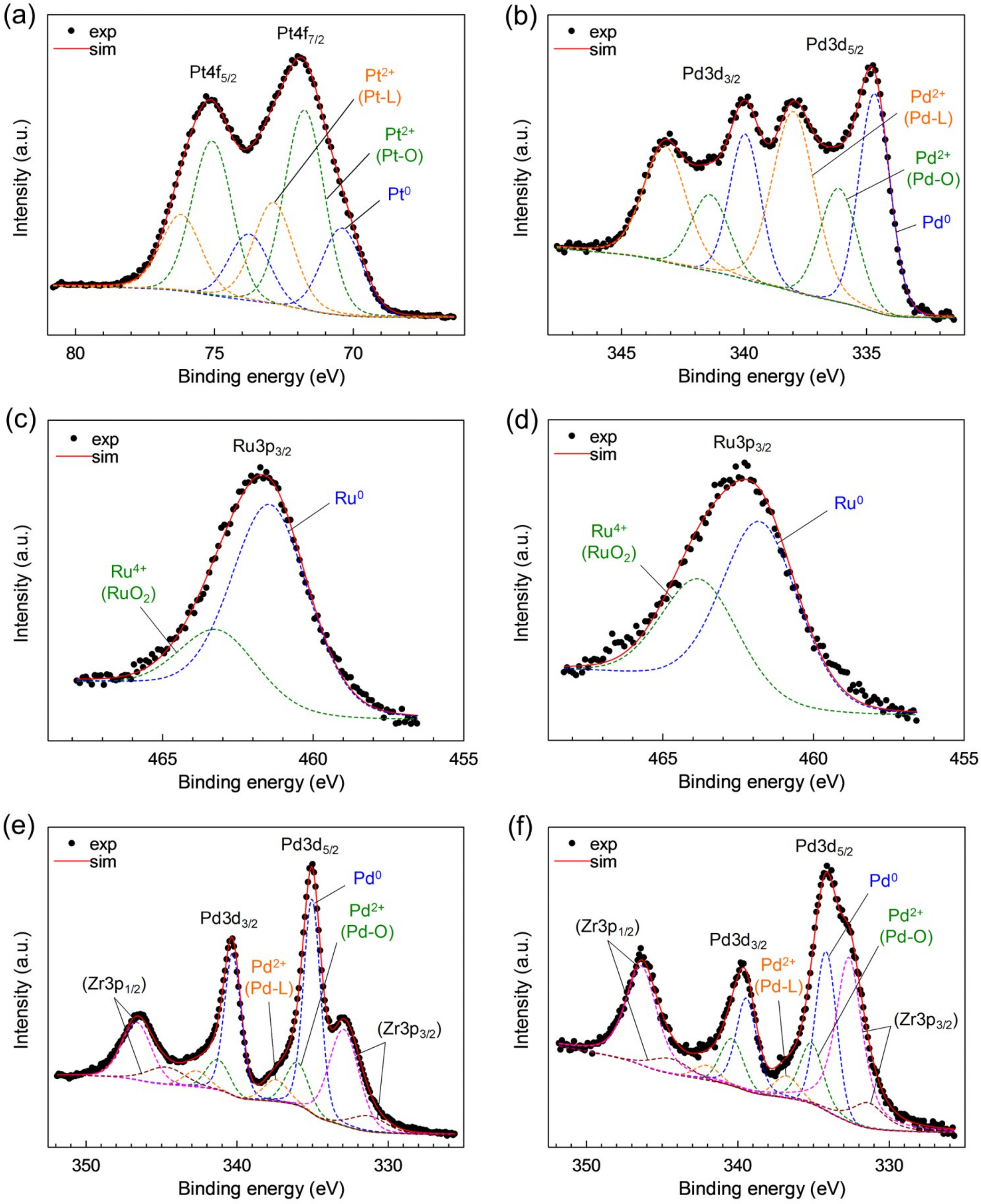

Fig. S11 XPS spectra of (a) **Pt/ZIF-8**, (b) **Pd/ZIF-8**, (c) **Ru/ZIF-8**, (d) **Ru/MIL-101**, (e) **Pd/UiO-66-NH$_2$**, and (f) **Pd-PVP/UiO-66-NH$_2$**. (L: ligand)

Table S2 Binding energies (BE) of core levels of **M/MOFs**.

Sample	Peak	BE (eV)	Relative peak area (%)
Pt/ZIF-8	Pt4$f_{7/2}$	70.4	21.7
		71.8	51.0
		72.9	27.3
Pd/ZIF-8	Pd3$d_{5/2}$	334.7	35.7
		336.1	22.1
		338.0	42.2
Ru/ZIF-8	Ru3$p_{3/2}$	461.3	75.9
		463.0	24.1
Ru/MIL-101	Ru3$p_{3/2}$	461.6	62.8
		463.6	37.2
Pd/UiO-66-NH$_2$	Pd3$d_{5/2}$	335.0	70.7
		336.0	18.8
		337.4	10.5
Pd-PVP/UiO-66-NH$_2$	Pd3$d_{5/2}$	334.2	60.4
		335.1	29.7
		336.8	9.9

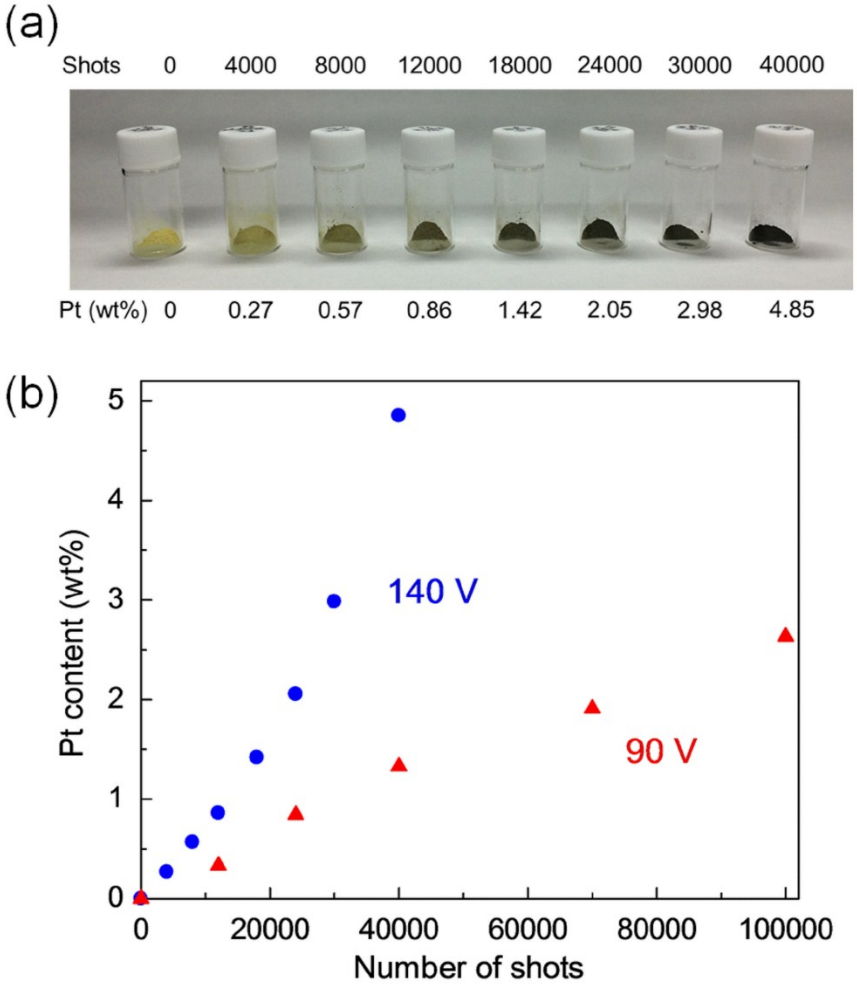

Fig. S12 (a) Photos of samples of **Pt^n/Zn-MOF-74** (shot number *n* = 0, 4000, 8000, 12000, 18000, 24000, 30000, and 40000) prepared at the applied voltage of 140 V. (b) Relation between number of shots and Pt content of the samples prepared at (blue) 140 V and (red) 90 V, estimated by ICP-AES measurements.

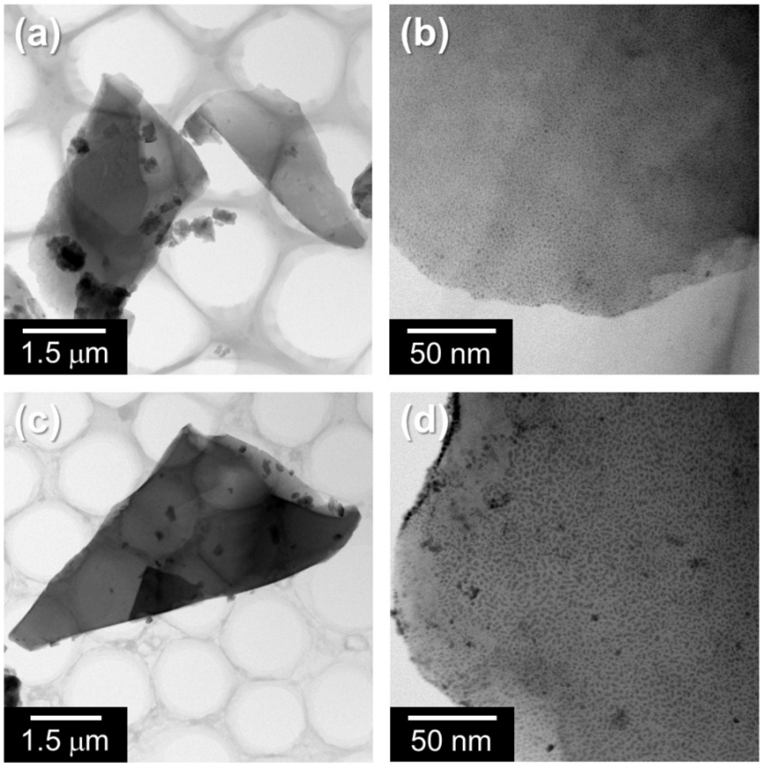

Fig. S13 STEM images exemplified by (a, b) **Pt^{12000}/Zn-MOF-74** and (c, d) **Pt^{24000}/Zn-MOF-74** (prepared at 140 V).

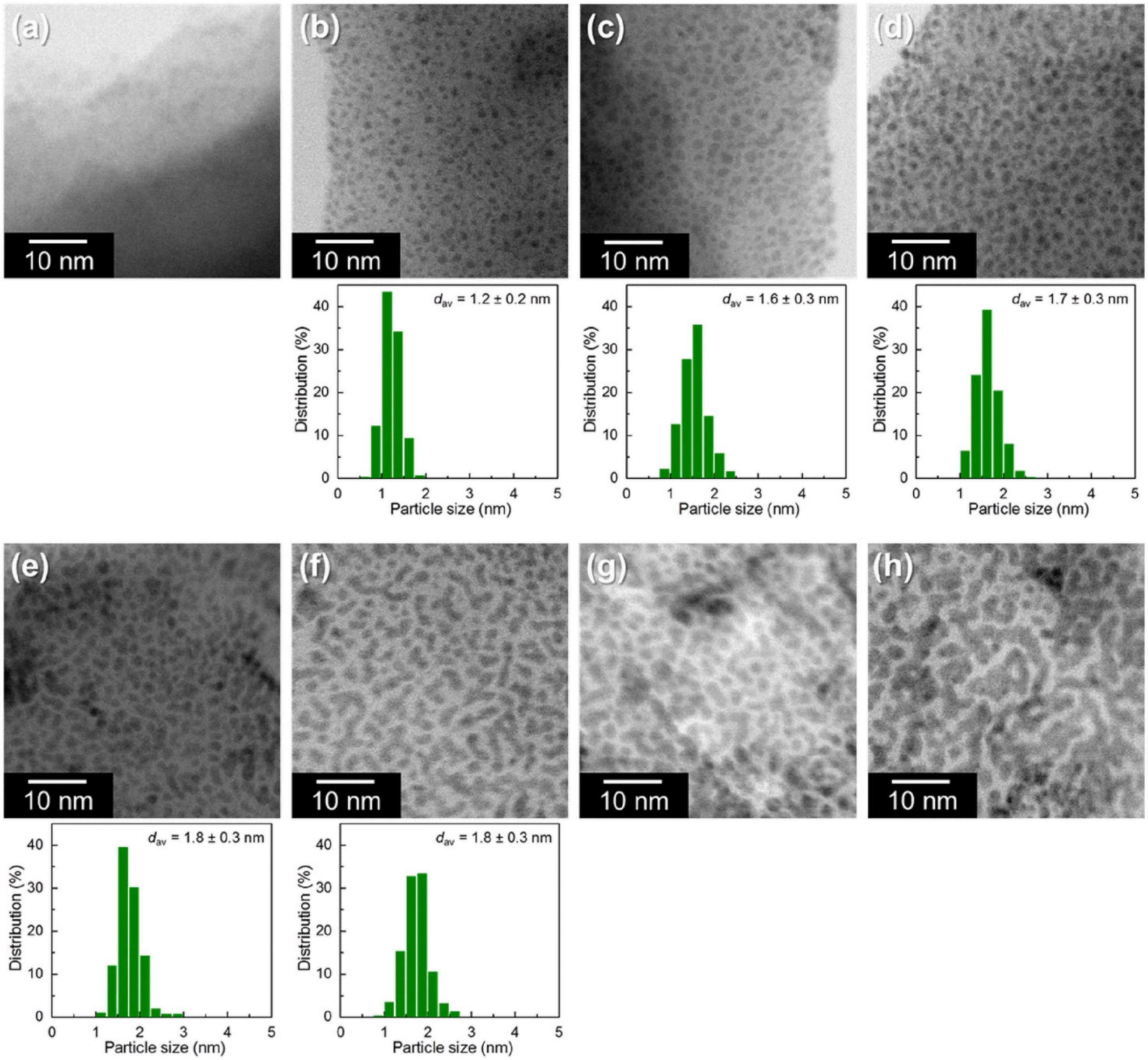

Fig. S14 Magnified STEM images and size distributions of spherical particles (calculated by counting only the spherical particles, rods or films were not counted) of (a) blank Zn-MOF-74, (b) **Pt^{4000}/Zn-MOF-74**, (c) **Pt^{8000}/Zn-MOF-74**, (d) **Pt^{12000}/Zn-MOF-74**, (e) **Pt^{18000}/Zn-MOF-74**, (f) **Pt^{24000}/Zn-MOF-74**, (g) **Pt^{30000}/Zn-MOF-74**, and (h) **Pt^{40000}/Zn-MOF-74**, prepared at 140 V.

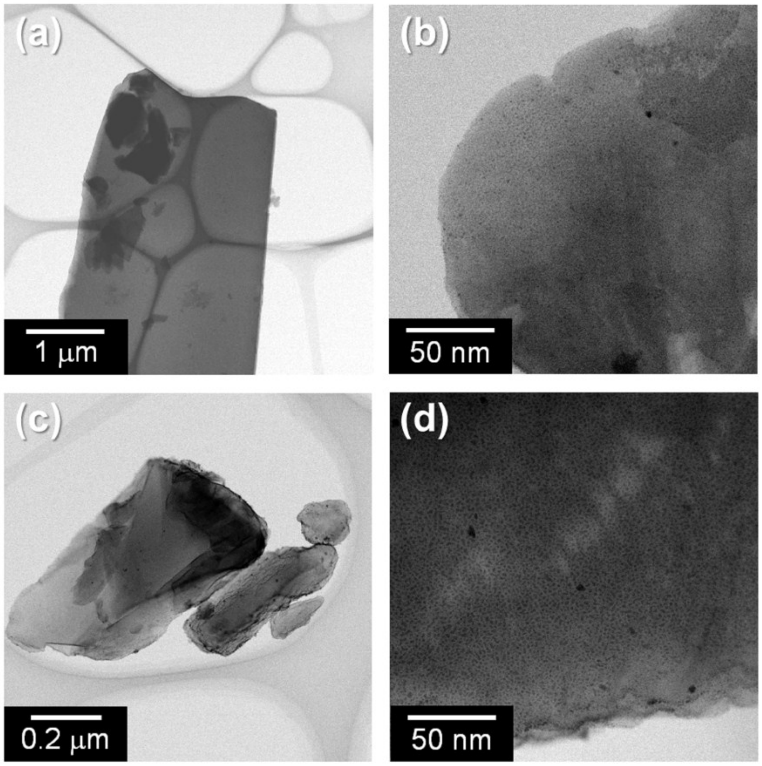

Fig. S15 STEM images exemplified by (a, b) **Pt^{24000}/Zn-MOF-74** and (c, d) **Pt^{70000}/Zn-MOF-74** (prepared at 90 V).

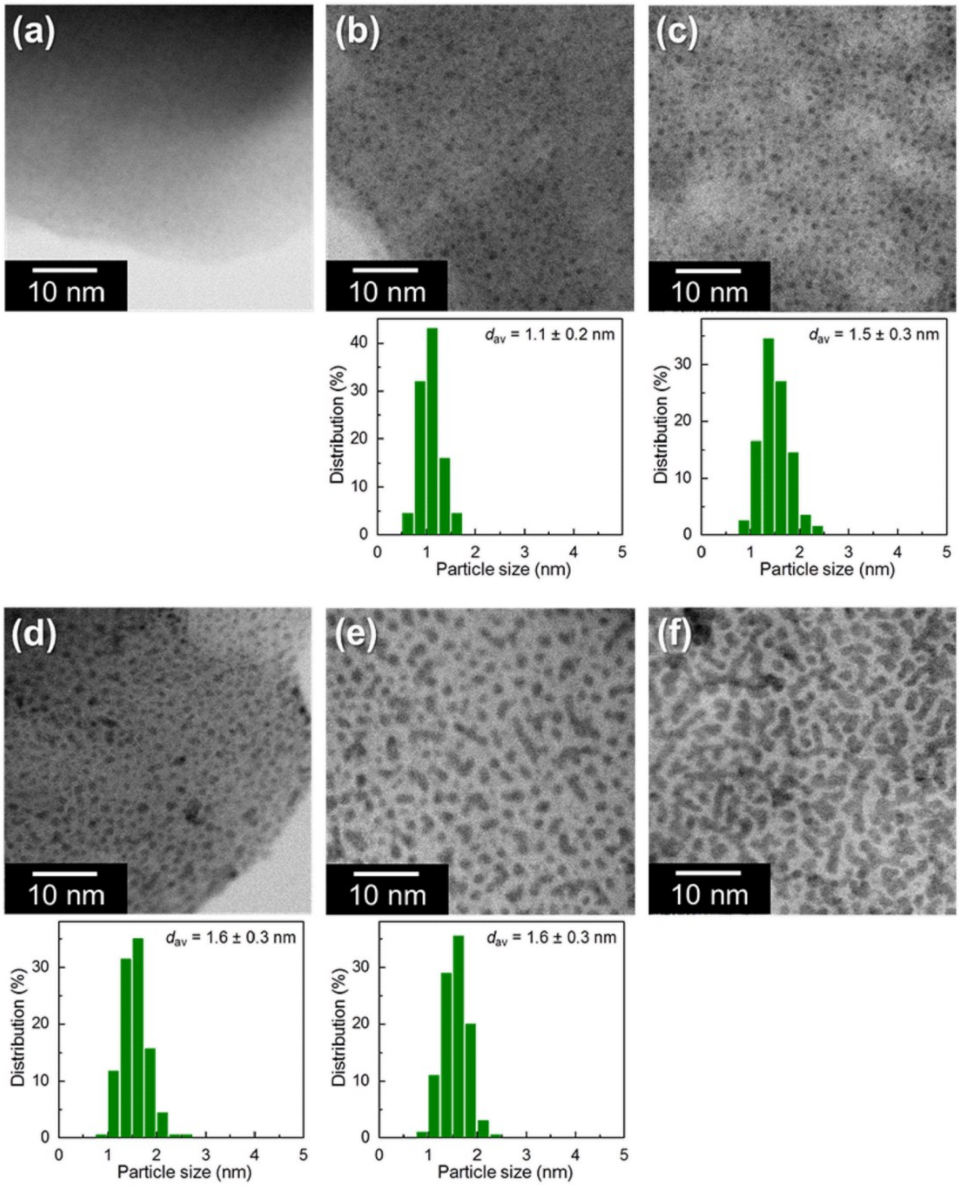

Fig. S16 Magnified STEM images and size distributions of spherical particles (calculated by counting only the spherical particles, rods or films were not counted) of (a) blank Zn-MOF-74, (b) **Pt^{12000}/Zn-MOF-74**, (c) **Pt^{24000}/Zn-MOF-74**, (d) **Pt^{40000}/Zn-MOF-74**, (e) **Pt^{70000}/Zn-MOF-74**, (f) **Pt^{100000}/Zn-MOF-74**, prepared at 90 V.

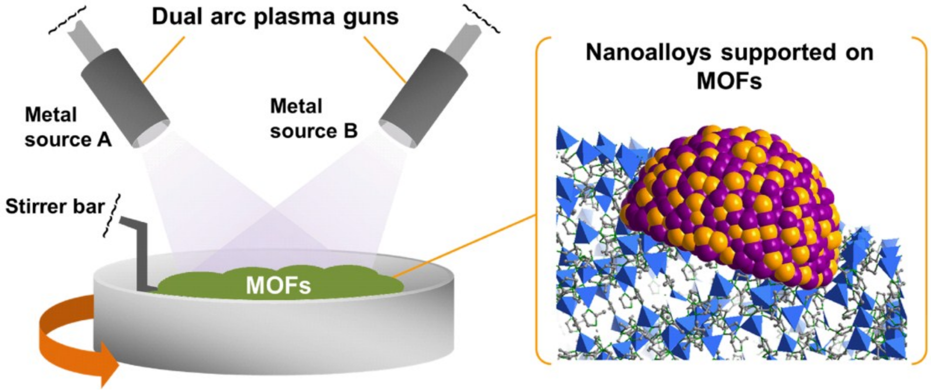

Fig. S17 Schematic illustration of the experimental settings for alloy synthesis on MOF supports with the APD method.

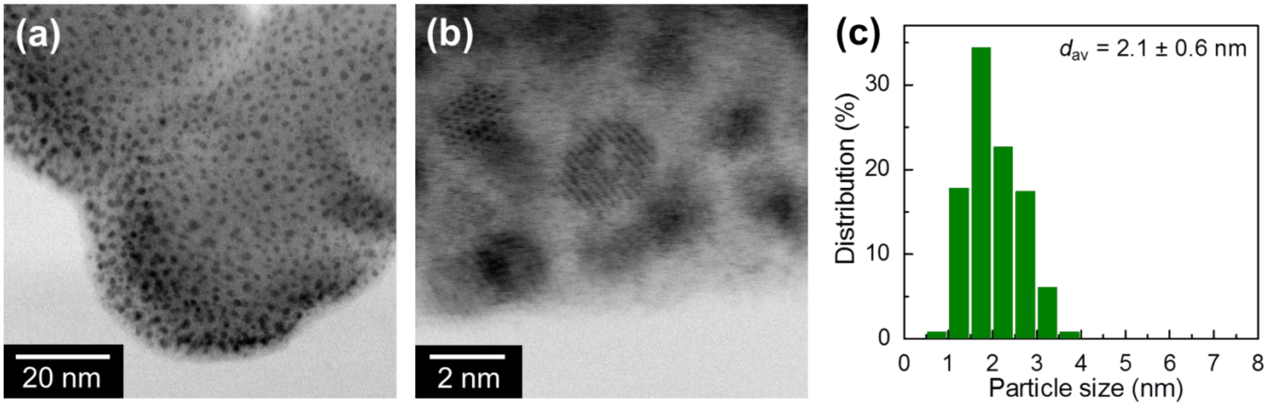

Fig. S18 (a) STEM image, (b) HR-STEM image, and (c) size-distribution of **Pt–Co/ZIF-8**.

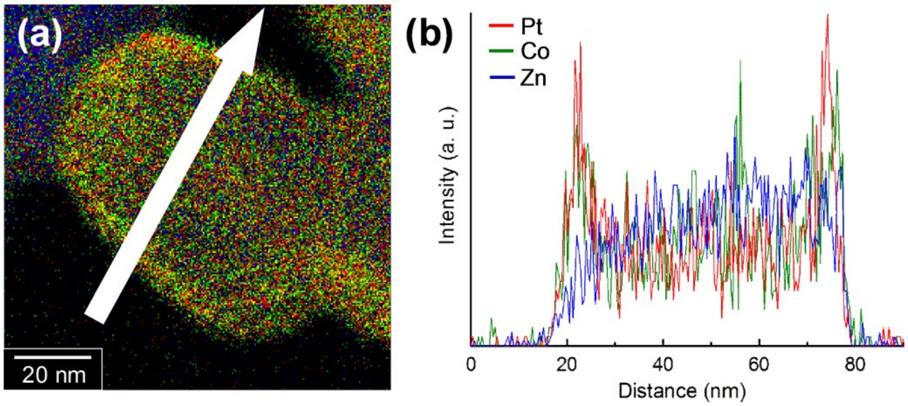

Fig. S19 (a) STEM–EDS map of **Pt–Co/ZIF-8**. (b) Line profiles along the arrow described in the STEM–EDS map. Red, green, and blue correspond to EDS signals from Pt-M, Co-K, and Zn-K, respectively.

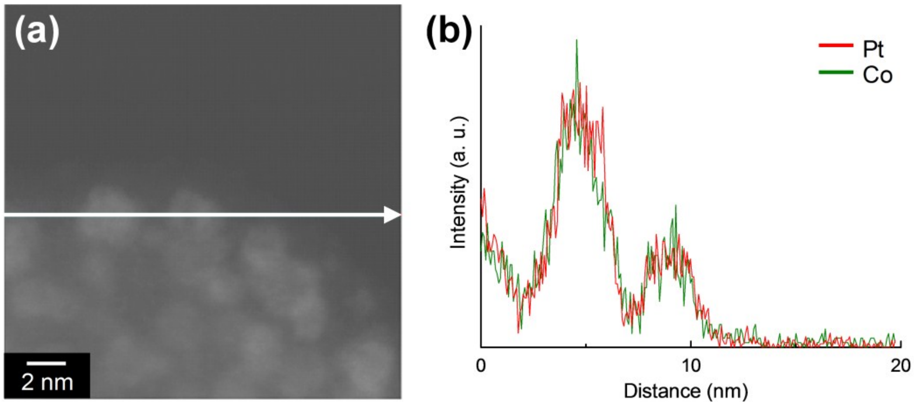

Fig. S20 (a) A magnified HAADF–STEM image of **Pt–Co/ZIF-8**. (b) Line profile of STEM–EDS analysis along the arrow in the left figure. Green and red correspond to Co-K and Pt-M, respectively.